Behavior of CFCC and CFRP Leadline Prestressing Systems in Bridge Construction

Nabil F. Grace, Ph.D., P.E.
Professor and Chairman
Civil Engineering Department
Lawrence Technological University
Southfield, Michigan

Tsuyoshi Enomoto
Engineer
Bridge and Structural Cable Department
Engineering Division
Tokyo Rope Mfg. Co., Ltd.
Tokyo, Japan

Kensuke Yagi
Manager, Engineering
Construction Materials Division
Mitsubishi Chemical Functional Products Inc.
Tokyo, Japan

Two commercially available carbon fiber reinforced polymer (CFRP) prestressing systems were compared for use in continuous prestressed concrete bridges in this investigation. Two two-span double-tee (DT) continuous bridge models were fabricated, instrumented, and tested. The two bridge models were identical except that Bridge Model CDT1 was pretensioned and post-tensioned with the CFRP Leadline™ tendon system, whereas the carbon fiber composite cable (CFCC)™ system was used in Bridge Model CDT2. The study examined parameters such as midspan deflections, concrete strains, and post-tensioning forces in externally draped strands/tendons under static loading and 15 million cycles of repeated loads. The ductility, failure modes, load carrying capacities, and post-tensioning tendon forces of both bridge models were compared by conducting an ultimate load test. The responses of both bridge models were almost identical, except for the failure mode and the ductility index.

Non-corrodible carbon fiber reinforced polymers (CFRPs) are currently being used in the construction of small and large-scale structures such as bridges.[1-5] Early research has shown that internally bonded tendons, in combination with externally draped unbonded tendons, can lead to reasonably ductile simply supported and continuous bridge systems.[6-8]

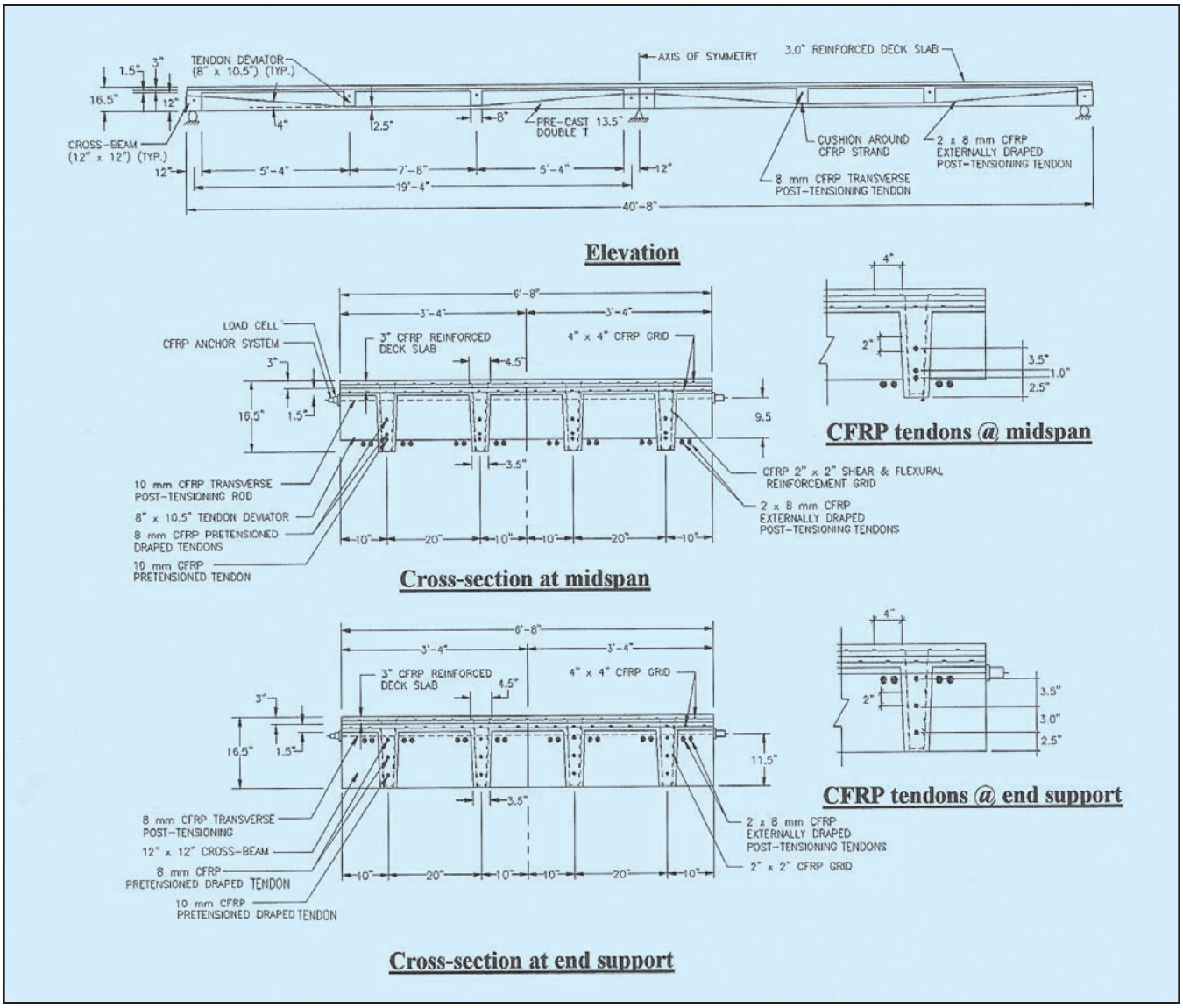

Fig. 1. Details of Bridge Model CDT1, prestressed using CFRP Leadline tendons and reinforced with NEFMAC grids.

Recently, Grace[8] experimentally investigated the response of a two-span continuous prestressed concrete bridge (Model CDT1), internally and externally prestressed using CFRP Leadline™* tendons.[9] The present investigation is an extension of the previous work[8] and aims to compare the response of Bridge Model CDT1 to a similar two-span continuous prestressed concrete bridge (Model CDT2), prestressed with carbon fiber composite cable (CFCC)™† strands.

In the previous investigation,[8] the overall deflection and strain responses of Model CDT1 were examined under static and repeated loads. The presence of continuous externally draped CFRP Leadline™ tendons (in the positive and negative moment regions), along with CFRP grids (NEFMAC[10]), resulted in a ductile continuous bridge system.

TEST PROGRAM

The current bridge model, designated as CDT2 (continuous double tee bridge, Model No. 2) is identical to Model CDT1, except for the type of prestressing system, flexural reinforcement, and shear reinforcement. The CFCC strands with built-in anchors (using a resin filling system) were used for prestressing Model CDT2 and its DT girders, while the CFRP Leadline tendons with a mechanical anchoring system were used for prestressing Model CDT1 and its DT girders. Also, CFCC stirrups were used for shear reinforcement in the DT girders of Model CDT2, while NEFMAC grids were used for flexural and shear reinforcement in Model CDT1.

Model CDT2 was fabricated in the same manner as Model CDT1. For the sake of completeness, construction details are also provided here. Model CDT2 consists of the following elements:

1. Precast concrete double tee (DT) girders prestressed with straight and internally draped bonded CFCC 1 x 7 strands.

2. Transverse unbonded CFCC 1 x 7 strands post-tensioned through tendon

* Manufactured by Mitsubishi Chemical Corporation, Japan.

† Manufactured by Tokyo Rope Mfg. Co., Ltd., Japan.

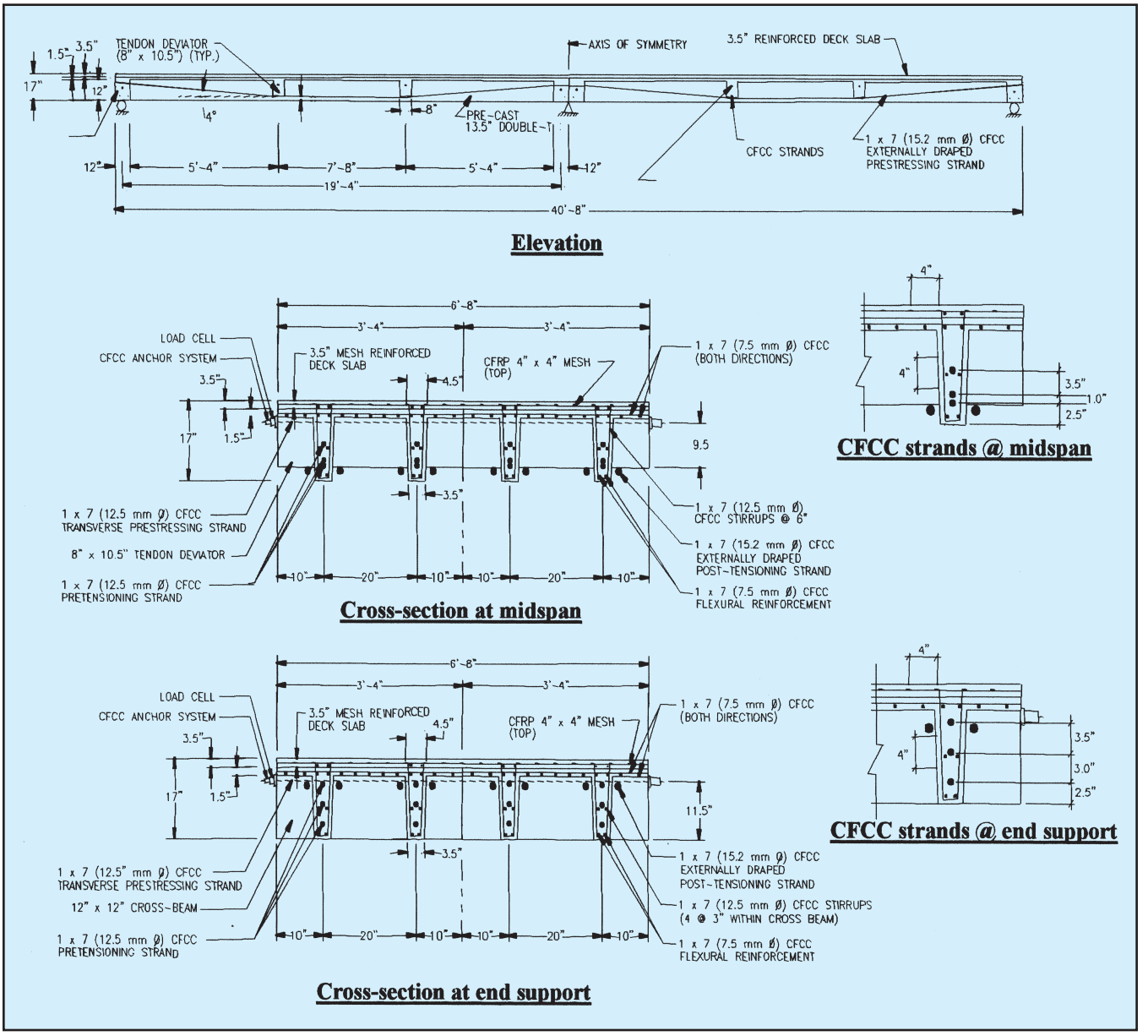

Fig. 2. Details of Bridge Model CDT2, prestressed and reinforced using CFCC strands.

deviators and cross-beams.

3. CFRP NEFMAC reinforced concrete deck slab.

4. CFCC 1 x 7 longitudinal and transverse reinforcements in flanges of DT girders, and CFCC 1 x 7 stirrups in webs and cross-beams/tendon deviators.

5. Continuous externally draped CFCC 1 x 7 strands.

Fabrication details and dimensions of Models CDT1 and CDT2 are shown in Figs. 1 and 2, respectively. Hold-up and hold-down devices[11] were used to develop the desired draped profile of the internal CFRP Leadline tendons and CFCC strands.

Construction Details

Four double tee (DT) girders, designated as CDT2-1, CDT2-2, CDT2-3 and CDT2-4, were fabricated and prestressed with CFCC strands. The characteristics and details of the CFRP Leadline tendons and the CFCC strands are given in Table 1.

In the above notation, CDT stands for continuous double tee. The number 2 refers to the type of strand (CFCC, in this case), and the last digit identifies the DT girder model number. Tendon deviators (located at approximate quarter points of each span) and cross-beams (located at each support) are integral parts of the DT girders.

The dimensional properties of each girder are summarized below:

- Span length: 19.33 ft (5.89 m)
- Girder depth: 13.5 in. (345 mm)
- Flange width: 40 in. (1015 mm)
- Distance between webs, center to center: 20 in. (510 mm)
- Flange thickness: 1.5 in. (38 mm)
- Web width, bottom: 3.5 in. (90 mm)
- Web width, at flange: 4.5 in. (115 mm)

Six strands per DT girder were tensioned prior to placing the concrete. Details of the prestressing, formwork, and other related fabrication procedures for the DT girders can be found in Reference 11.

Table 1. Characteristics of Leadline tendons and CFCC strands.

Characteristic	CFRP Leadline tendons	CFCC strands
Matrix	Epoxy	Epoxy
Carbon fiber volume fraction, percent	65	65
Tensile strength, ksi (kN/mm^2)	328 (2.25)	272 (1.88) for 7.5 mm diameter strand 271 (1.87) for 12.5 mm diameter strand 254 (1.75) for 15.2 mm diameter strand
Young's modulus, ksi (GPa)	21,320 (147)	19,865 (137)
Extension at break, percent	1.5	1.6
Thermal expansion, 1/°C	0.6 x 10^{-6}	0.6 x 10^{-6}
Effective cross-sectional area, sq in. (mm^2)	0.071 (46.1) for 8 mm diameter tendon 0.111 (71.8) for 10 mm diameter tendon	0.047 (30.4) for 7.5 mm diameter strand 0.118 (76.0) for 12.5 mm diameter strand 0.176 (113.6) for 15.2 mm diameter strand
Guaranteed tensile strength, kips (kN)	23.4 (104) for 8 mm diameter tendon 36.4 (162) for 10 mm diameter tendon	12.81 (57) for 7.5 mm diameter strand 31.92 (142) for 12.5 mm diameter strand 44.74 (199) for 15.2 mm diameter strand

Note: 1 in. = 25.4 mm; 1 ksi = 0.006895 kN/mm^2 = 0.006895 GPa.

Reinforcement Details in DT Girders

The flexural and shear reinforcement in Model CDT1 girders consisted of NEFMAC two-dimensional grids in a three-dimensional CFRP cage arrangement.[11] However, the flexural reinforcement in the flange of the DT girders of Model CDT2 consisted of 0.3 in. (7.5 mm) diameter CFCC strands placed in the longitudinal and transverse directions.

The longitudinal flexural reinforcement was spaced at 3 in. (76 mm), while the transverse flexural reinforcement was spaced at 6 in. (152 mm). The web reinforcement of Model CDT2 girders consisted of 0.5 in. (12.5 mm) CFCC stirrups at a spacing of 6 in. (152 mm).

In addition, four CFCC strands, each 0.5 in. (12.5 mm) in diameter, were provided on each side face of the webs for flexural reinforcement. The details of the flexural and shear reinforcement in the DT girders of Models CDT1 and CDT2 can be found in Reference 11.

Pretensioning and Release of Prestressing Force

The desired draped profile in the top two Leadline tendons (see Fig. 1) and CFCC strands (see Fig. 2) was achieved using hold-up and hold-down devices. Each tendon/strand was pretensioned by a hydraulic jack and appropriate compatible devices.[11] The average prestressing force in the CFCC draped strands was 16.7 kips (74.3 kN), while in the straight CFCC strands, the average prestressing force was 16.5 kips (73.4 kN).

This resulted in an average stress of 142 ksi (979 MPa) in the draped tendons and 140 ksi (965 MPa) in the straight tendons. The range of the prestressing force varied from 47 to 59 percent of the guaranteed strength of the CFCC strands, compared to 60 to 70 percent of the guaranteed strength of the CFRP Leadline tendons.

In Model CDT1, the average prestressing forces in the draped [0.3 in. (8 mm)] and straight [0.4 in. (10 mm)] tendons were about 17 and 19 kips (76 and 85 kN), respectively. These prestressing forces resulted in average stresses of 239 and 170 ksi (1650 and 1170 MPa) in the 0.3 and 0.4 in. (8 and 10 mm) diameter CFRP Leadline tendons, respectively.

The strands were released using a hand-held saw at both ends. First, the top pair of strands (one in each web) was simultaneously released at both the live and dead ends. Next, the second pair of strands was released. The bottom strands were released last. Details of this procedure can be found in Reference 11.

Construction of Bridge Model CDT2

Model CDT2 was fabricated in the same manner as Model CDT1.[8] Each of the four precast CDT2 girders was transported to the testing area and positioned over the supports as a simply supported girder. The gap at the joints between the DT girders was filled with Sikadur 30 epoxy grout.[12]

The bridge model was 6.66 ft (2.030 m) wide. Each span was 19.33 ft (5.890 m) long. Continuous externally draped 0.6 in. (15.2 mm) diameter CFCC strands were used for the external post-tensioning of the bridge model. One strand was placed on each side of each web. Identical strands were used for transverse post-tensioning (see Fig. 2).

Post-tensioning forces were applied in two stages. In the first stage, prior to casting the deck slab, 10 and 50 percent of the desired post-tensioning forces in the continuous externally draped CFCC strands and in the transverse prestressing strands were applied, respectively.

Partial prestressing in the longitudinal and transverse directions was applied to ensure that the four DT girders formed a tight platform for the deck slab. Cushioning materials were placed between the strands and the concrete at the tendon deviators and at the cross-beams to ensure the successful performance of the continuous externally draped strands.[7]

The form of the deck slab was assembled and NEFMAC grids[11] [4 x 4 in. (100 x 100 mm) spacing] to be used as flexural reinforcement were placed in the form. The same concrete mix that was used in the construction of the DT girders [compressive strength of 7 ksi (48 MPa)] was used in the construction of the deck slab.

After curing the deck slab, the externally draped continuous strands were retensioned to the desired prestressing force of 18.6 kips (82.8 kN) per strand. The post-tensioning forces in

Fig. 3. Post-tensioned continuous externally draped CFRP Leadline tendons (shown from below), Bridge Model CDT1.

the transverse direction were also increased, for a total force of 10 kips (45 kN) per strand.

A typical arrangement of the external CFRP Leadline tendons (Model CDT1) after post-tensioning is shown in Fig. 3. Note that the initial post-tensioning forces were readjusted (increased) [after 7.5 million cycles of repeated loads] during the testing stage of both bridge models.

Fig. 4 shows the post-tensioning arrangement of the externally draped CFCC strands. Average values of the post-tensioning forces (initial and adjusted), stresses, and elongation in each pair of external prestressing Leadline tendons and in a single CFCC strand (placed on each side of each web) are listed in Table 2.

Instrumentation and Loading Setup

A four-point loading system, resembling the front and the rear axles of a truck, was used to apply static and repeated loads to the bridge models using load controlled MTS actuators. Fig. 5 shows Model CDT2 under two repeated loads. As in the case of Model CDT1,[8] repeated loads were applied at the midspans of Model CDT2.

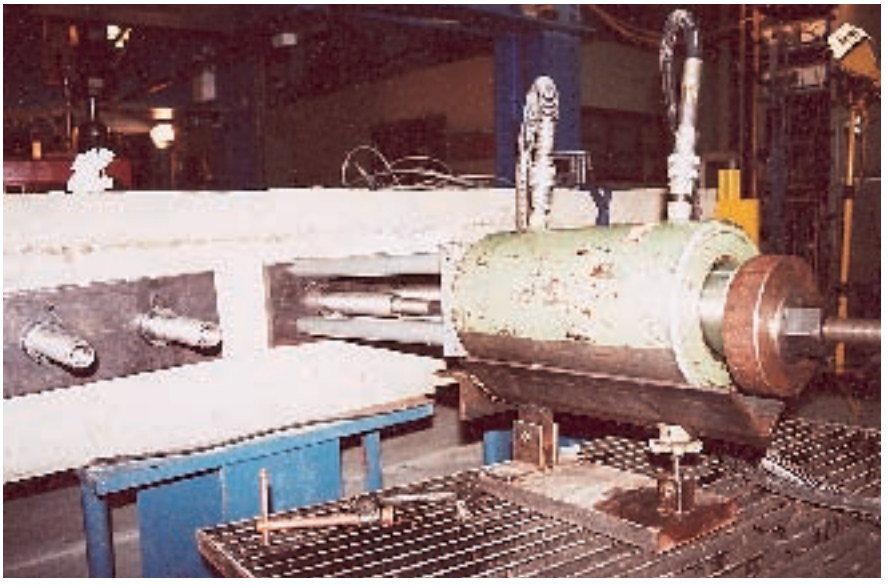

Fig. 4. Post-tensioning of an externally draped CFCC strand, Bridge Model CDT2.

Midspan 1 was subjected to a repeated load of 19 kips (84.6 kN) amplitude, while a repeated load of 40 kips (178 kN) amplitude was used at Midspan 2. The lighter and heavier repeated loads were selected to simulate approximately one and two times the service load, respectively. The lighter load ranged from 2 to 21 kips (8.9 to 93.5 kN), while the heavier load ranged from 5 to 45 kips (22.3 to 200.3 kN).

The two repeated loads were applied to determine if there was any adverse effect of a repeated load on the bridge model, and to investigate ways to regain the strength of the bridge, which was overloaded under the heavier load. The frequency of repeated loads was 2.5 Hz.

As in the case of Model CDT1,[8] after every million cycles, a static load test was conducted to obtain deflections, strains, and post-tensioning forces in the continuous externally draped strands and the transverse CFCC strands. These parameters were recorded at each increment/decrement of 5 kips (22.3 kN) during the loading/unloading of the static loads.

Load cells attached at the dead ends monitored post-tensioning forces in the continuous external strands and the transverse strands. The deflection measurements were taken using linear motion transducers (LMT) attached along the length of both spans, and along their width at midspans, while strain measurements were made with electrical resistance strain gauges.

DISCUSSION OF TEST RESULTS

Figs. 6(a) and 6(b) show the strain distributions at Midspan 2 and at the intermediate support after post-tensioning of Models CDT1 and CDT2, respectively. The tensile strain at the flange top (at Midspan 2) of Model CDT2 [Fig. 6(b)] is 4.8 times that of Model CDT1, while the compressive strain at the web bottom is 17.8 percent lower than that of Model CDT1.

At the intermediate support of Model CDT2, the compressive strain at the top of the flange and the tensile strain at the bottom of the web are 4 percent lower and 17.3 percent higher,

Table 2. Average post-tensioning forces in continuous externally draped CFRP Leadline tendons and CFCC 1 x 7 strands.

Post-tensioning tendon/strand type	Initial post-tensioning at zero cycles			Adjusted (increased) post-tensioning force at 7.5 million cycles		
	Post-tensioning force kips (kN)	Stress ksi (MPa)	Elongation in. (mm)	Post-tensioning force kips (kN)	Stress ksi (MPa)	Elongation in. (mm)
CFRP Leadline tendon	17.5 (77.9)	122.6 (845.3)	2.8 (71)	23.1 (102.8)	161 (1110)	3.9 (99)
CFCC strand	18.6 (82.6)	105.4 (726.9)	3.0 (76)	23.2 (103.2)	132 (909)	3.9 (99)

Note: 1 in. = 25.4 mm; 1 kip = 4.448 kN; 1 ksi = 6.895 MPa.

respectively, than those of Model CDT1. Thus, it is observed that there is no significant difference in the strain distribution after post-tensioning of Models CDT1 and CDT2.

Note that the tension and/or compressive strain distribution remains the same for both bridge models at each construction stage. Small differences may be due to different levels of prestressing and stress transfer in the girders.

The effect of repeated loads with constant amplitudes of 19 and 40 kips (84.6 and 178 kN), acting at Midspan 1 and Midspan 2, respectively, on the post-tensioning forces in the external strands is shown in Figs. 7(a) and 7(b) for Models CDT1 and CDT2, respectively. After 7.5 million cycles of repeated loads, the post-tensioning forces were adjusted (increased) by an average of 5 kips (22.3 kN) per strand/tendon.

The post-tensioning adjustment resulted in a 31.5 percent increase in the post-tensioning force of each strand/tendon. Both bridge models were tested again for an additional 7.5 million cycles, for a total of 15 million cycles.

Note that this adjustment (increase) in the post-tensioning forces was intended to restore any loss in parameters such as deflection and strain, and to examine whether the life span of the bridge models could be increased

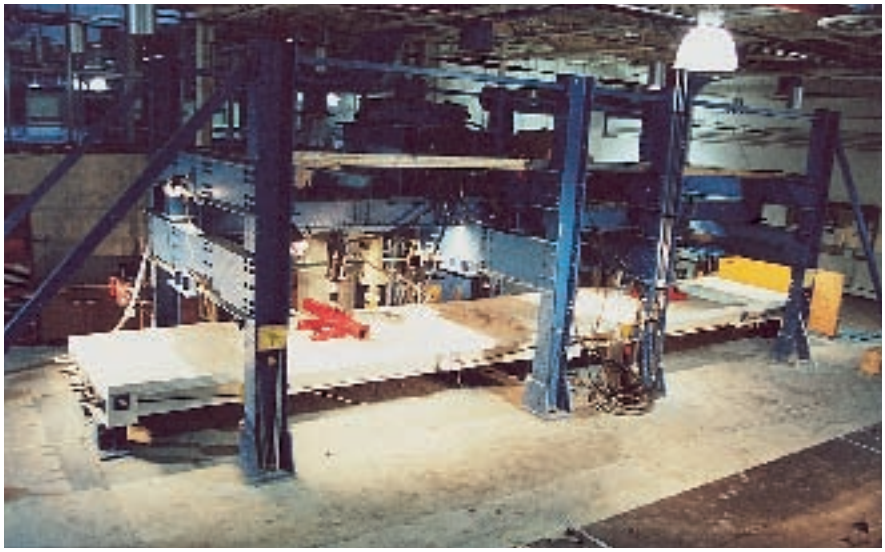

Fig. 5. Two-span continuous Bridge Model CDT2 under two repeated loads (one in each span).

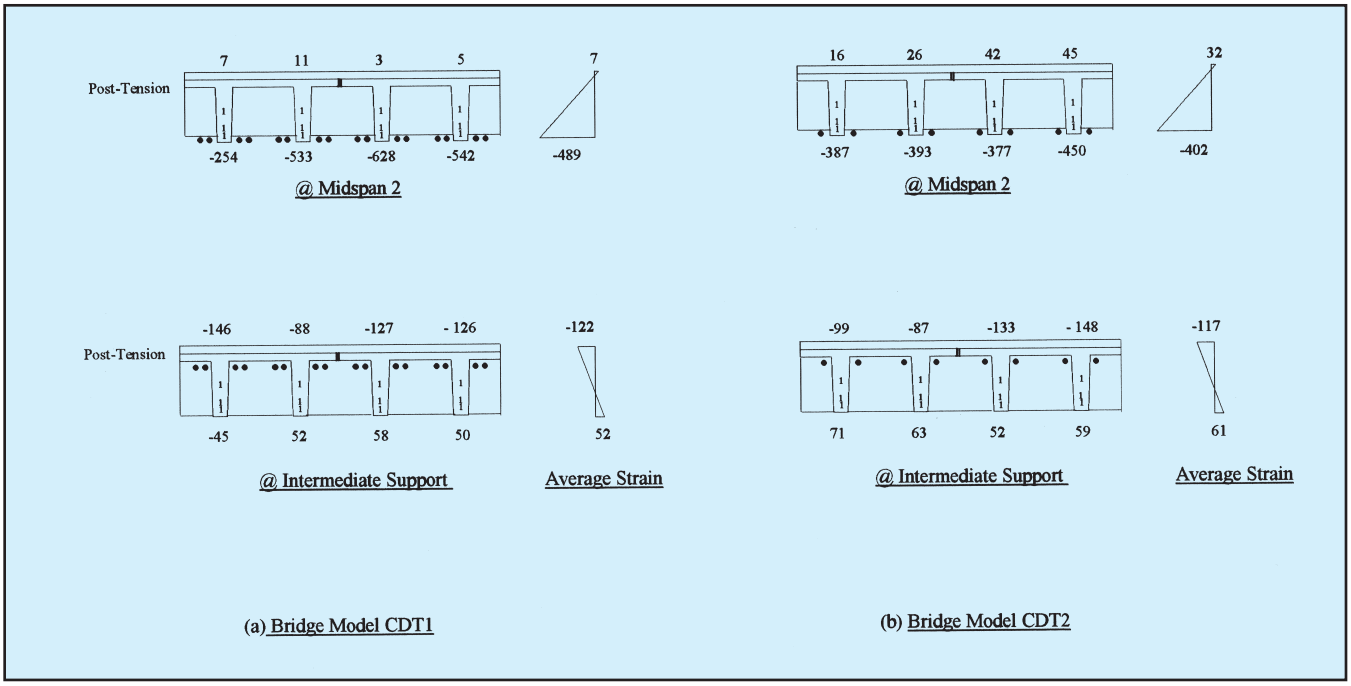

Fig. 6. Strain (micro in./in.) distribution in Bridge Models CDT1 and CDT2.

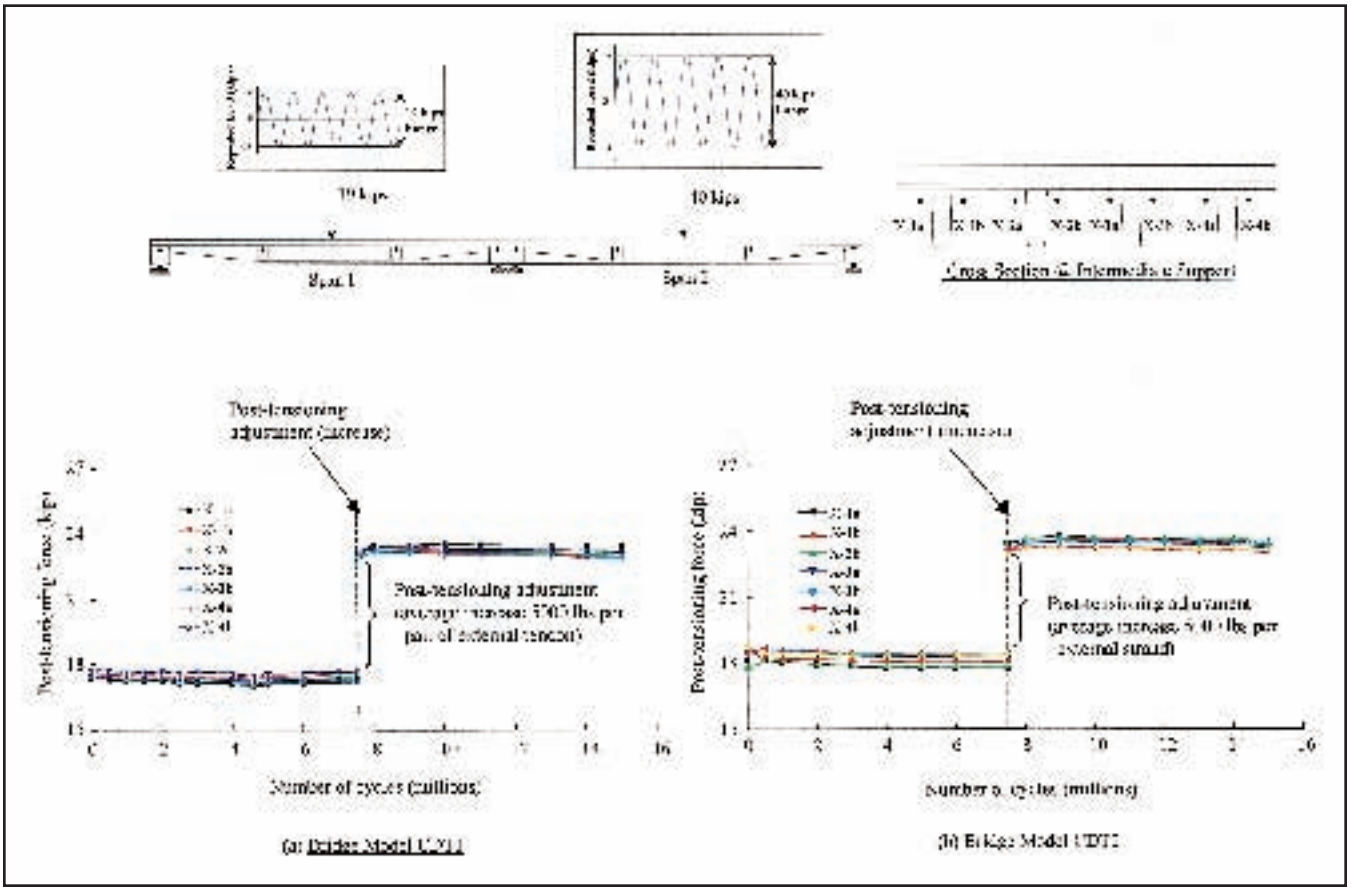

Fig. 7. Effect of repeated loads on continuous externally draped prestressing strands.

at a particular age of the bridge. Repeated load cycles have an insignificant effect on post-tensioning forces both before and after the post-tensioning adjustment in both bridge models.

Figs. 8 and 9 show the load versus post-tensioning force relationships in the external CFRP Leadline tendons and CFCC strands, respectively. The post-tensioning forces remain almost unchanged as the static load is applied, for both bridge models. However, the post-tensioning force in the Leadline tendons after the adjustment decreases (see Fig. 8) by about 13 percent after an additional 7.5 million cycles of repeated load is applied on the midspans. There is no corresponding reduction in the post-tensioning forces in the CFCC strands (see Fig. 9).

The load versus deflection relationships before and after the post-tensioning adjustment for zero, 7.5, and 15 million cycles are presented in Figs. 10 and 11 for Models CDT1 and CDT2, respectively. For both bridge models, there is no significant difference in the load versus deflection relationships, both before and after the post-tensioning adjustment for

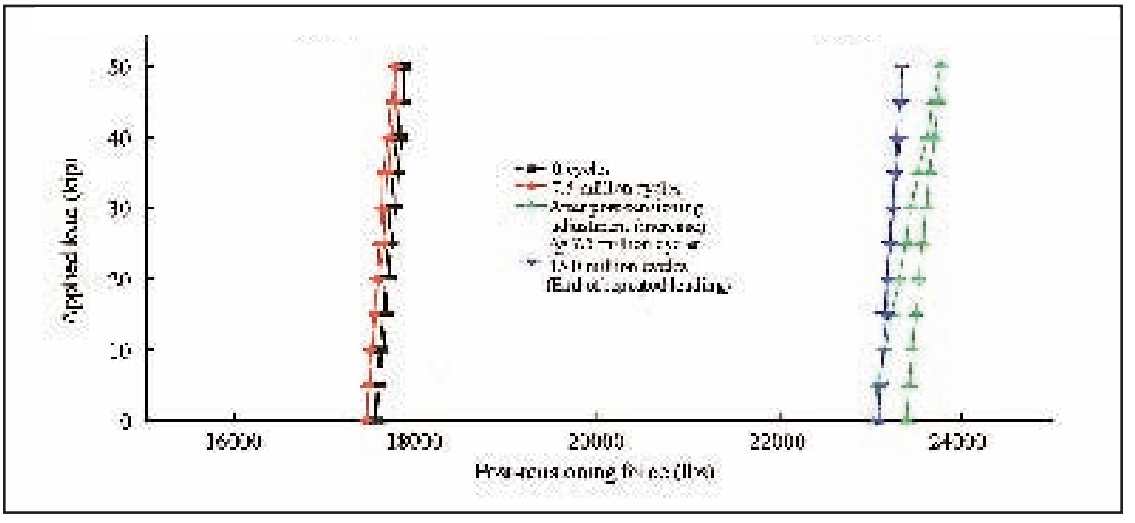

Fig. 8. Average post-tensioning forces due to static load in continuous externally draped CFRP Leadline tendons, Bridge Model CDT1.

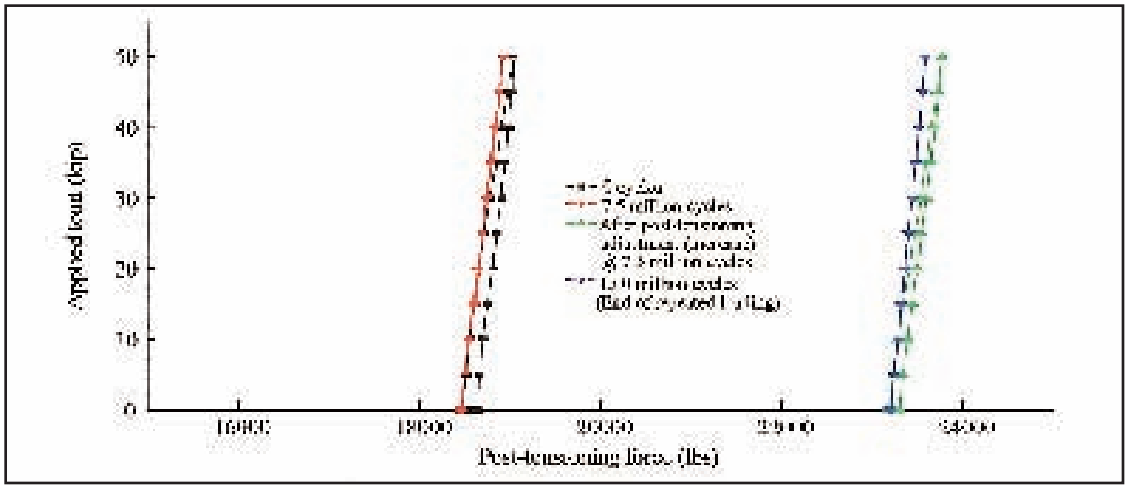

Fig. 9. Average post-tensioning forces due to static load in continuous externally draped CFCC strands, Bridge Model CDT2.

Midspan 1 and Midspan 2. This suggests that both prestressing systems are providing an almost identical response after exposure to 15 million cycles of the service load (Span 1) and twice the service load (Span 2).

The strain variations of Midspan 1 at the top of the deck slab and at the web bottom versus applied static load, before and after the post-tensioning adjustment, are shown in Figs. 12 and 13, respectively. The strain values of the deck slab of Model CDT2 after the post-tensioning adjustment at 7.5 million cycles are less than those before

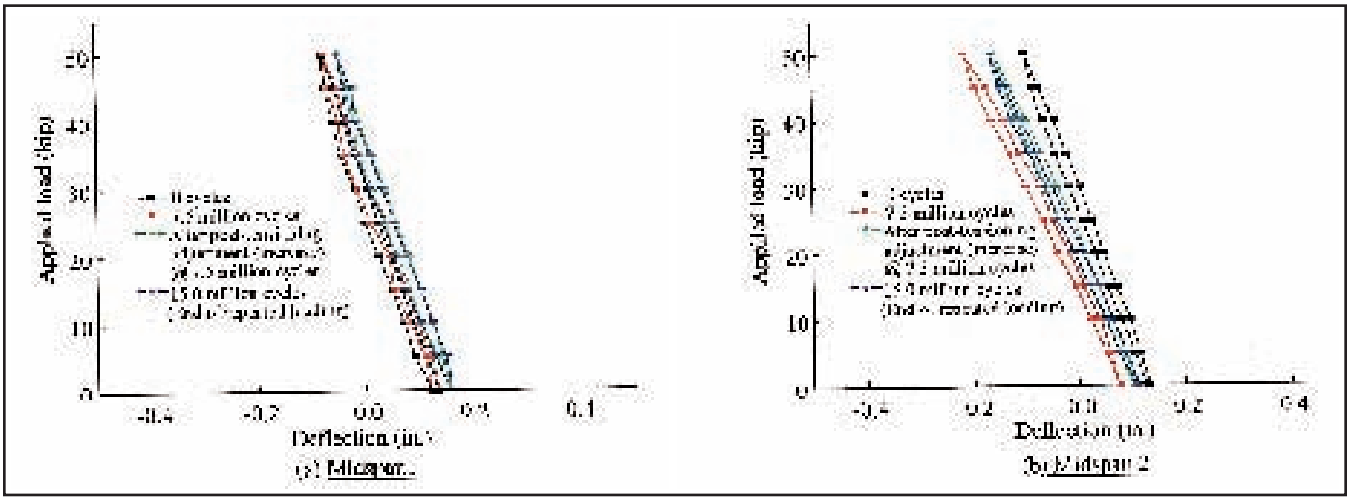

Fig. 10. Deflection at midspans due to static loads in Bridge Model CDT1.

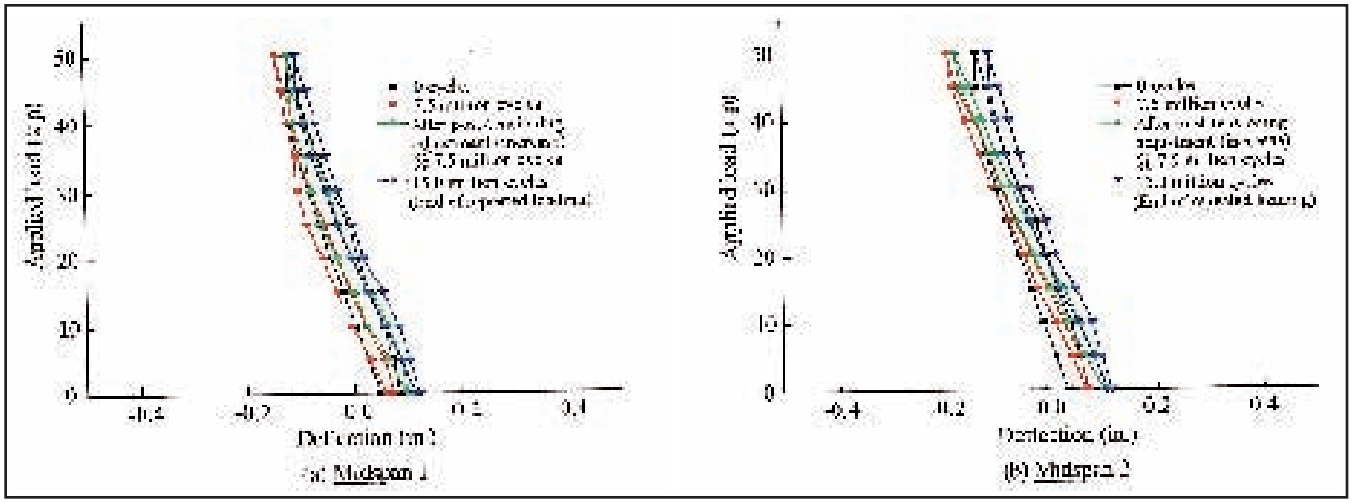

Fig. 11. Deflection at midspans due to static loads, Bridge Model CDT2.

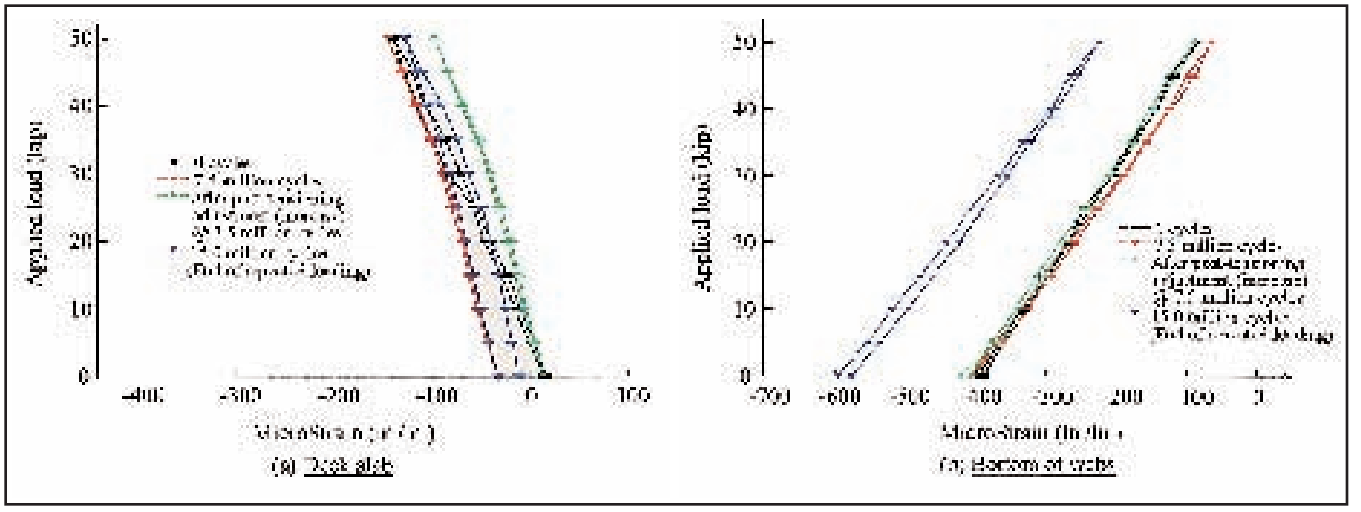

Fig. 12. Strain variation at Midspan 1 due to static loads, Bridge Model CDT1.

the post-tensioning adjustment. However, the compressive deck slab strains of Model CDT2 increase almost uniformly during an additional 7.5 million cycles for the whole range of applied static load.

The strain values (see Fig. 13) after the post-tensioning adjustment at the bottom of the webs of Model CDT2 are higher (in compression) than those before the post-tensioning adjustment, at the lower level of static loading. However, at the upper level of static loading [i.e., at 50 kips (222.3 kN)], the compressive strain values are reduced by about 80 percent.

As shown in Fig. 12(a), in the case of Model CDT1, the strain values at the deck slab for a specific value of load are highest before the post-tensioning adjustment and lowest after the post-tensioning adjustment. After 15 million cycles, the strain values are closer to those found at zero and 7.5 million cycles before the post-tensioning adjustment.

Therefore, the strain distribution in the deck is improved by the post-tensioning adjustment, even after an additional 7.5 million cycles of repeated loads. Fig. 12(b) shows that the compressive strain values after 15 million cycles of repeated loads are much larger than those corresponding to zero and 7.5 million cycles (before and after the post-tensioning adjustment).

Figs. 14 and 15 show the strain variation versus applied static loading at the intermediate supports of Models CDT1 and CDT2, respectively, after the application of zero, 7.5, and 15 million cycles of repeated loads. The strain values at the deck slab of Model CDT2 [Fig. 16(a)] are not significantly affected by the applied load, regardless of the number of repeated load cycles. However, for a specific load, strains at the deck slab for different numbers of repeated load cycles differ significantly from each other.

The highest strain is observed at 15 million cycles and the lowest at zero cycles. Also, the deck slab strain after the post-tensioning adjustment (at 7.5 million cycles) lies between the strains corresponding to zero and 7.5 million cycles (before the post-tensioning adjustment). This may be attributed to the development of transverse cracks at the intermediate support in the deck slab.

From Fig. 15(b), the strain in the web changed from tension to compression at higher values of static loading,

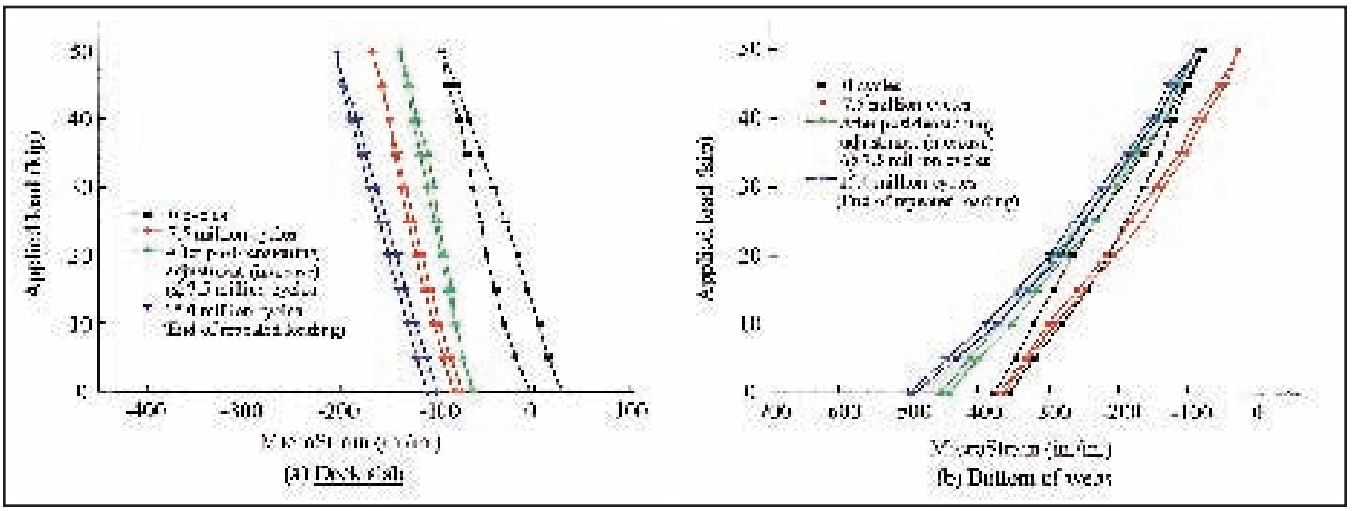

Fig. 13. Strain variation at Midspan 1 due to static loads, Bridge Model CDT2.

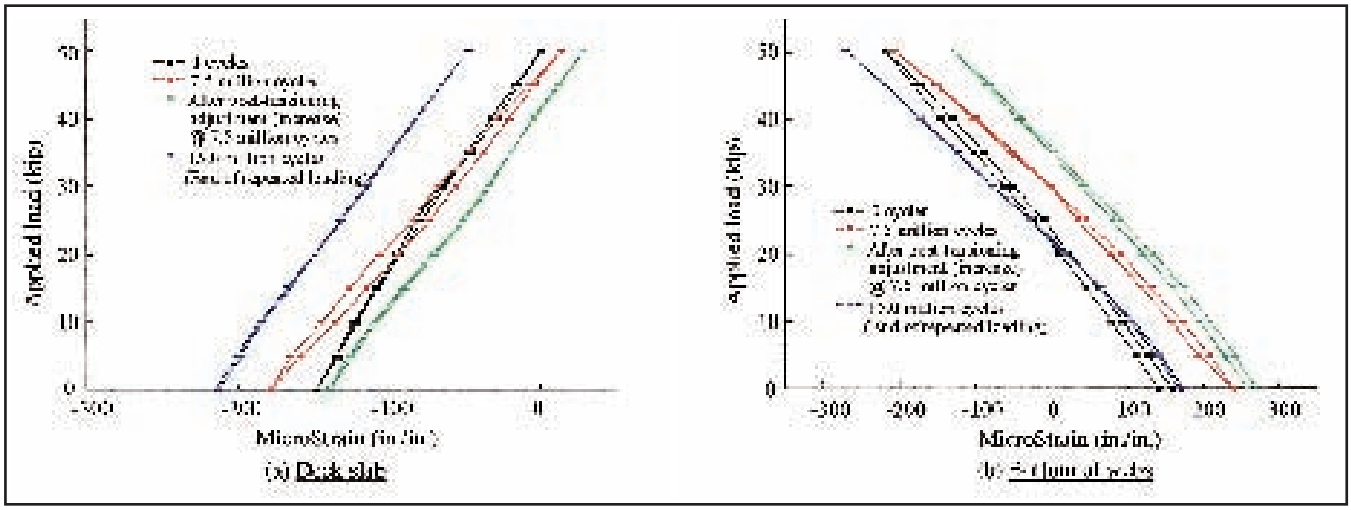

Fig. 14. Strain variation at intermediate support due to static loads, Bridge Model CDT1.

but showed no significant variation with the number of repeated load cycles. For a specific load, the compressive/tensile strain in the web is higher/lower before the post-tensioning adjustment at 7.5 million cycles than immediately after the post-tensioning adjustment.

Nonetheless, as shown in Fig. 14(a), in the deck slab of Model CDT1, the strain values at 7.5 million cycles after the post-tensioning adjustment are the lowest. Also, note that after the completion of repeated load cycles, i.e., after 15 million cycles, there is a significant change (about 40 percent) in the deck slab strain values from those at 7.5 million cycles after the post-tensioning force adjustment.

From Fig. 14(b), the load versus strain (at the bottom of the web) relationships for Model CDT1 differ significantly from those of Model CDT2. For a specific load, the web strain (tensile/compressive) immediately after the post-tensioning adjustment at 7.5 million cycles is higher/lower in comparison to the strain after 15 million cycles of repeated loads.

ULTIMATE LOAD TEST

To compare the failure characteristics of both bridge models, ultimate load tests were carried out. In these tests, the ultimate load carrying capacity, maximum deflection, critical failure section, failure mode, and variation in the post-tensioning forces in the continuous externally draped tendons/strands were examined and evaluated.

To determine the inelastic energies absorbed in Models CDT1 and CDT2, static loading and unloading tests were conducted. In these tests, the load was increased from zero to a maximum value of 60, 90, 100, 110, 120, 140, 160 kips (267, 400.5, 445, 489.5, 534, 623, 712 kN) and then unloaded to a zero load. Each loading/unloading cycle followed the same procedure.

The final load increased with each cycle until it approached the failure load of the bridge model. The failure load of Model CDT1 was 162 kips (720.9 kN), whereas the failure load of Model CDT2 was 167 kips (743.2 kN). The ductility ratio for Midspan 2 of Model CDT1 was 86 percent, while the corresponding ductility ratio for Model CDT2 was 69.5 percent.

The corresponding ductility ratios

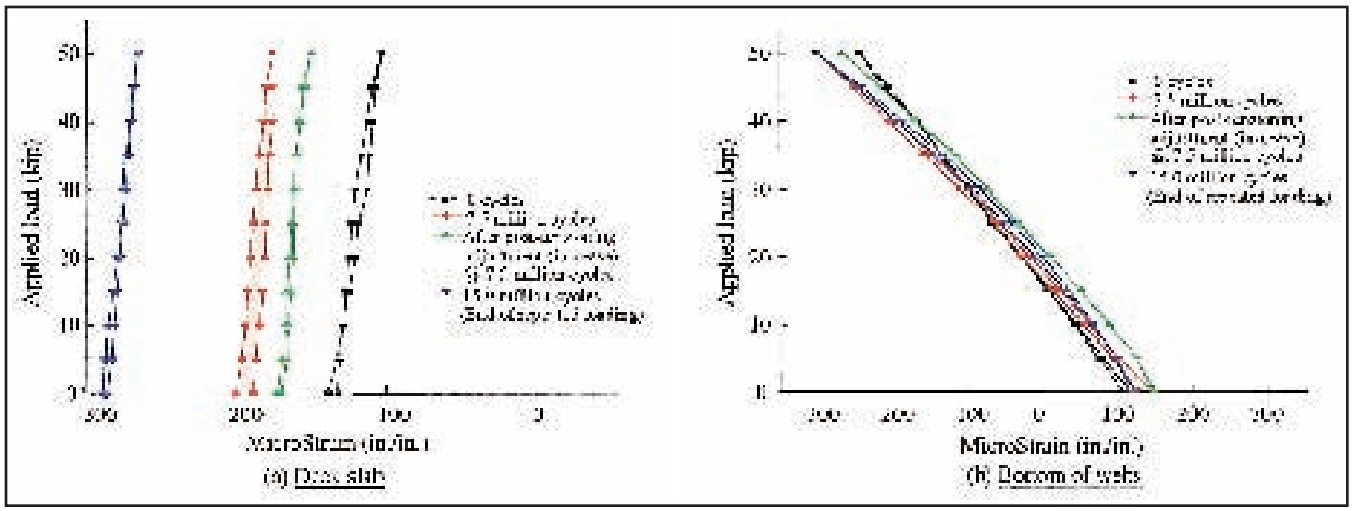

Fig. 15. Strain variation at intermediate support due to static loads, Bridge Model CDT2.

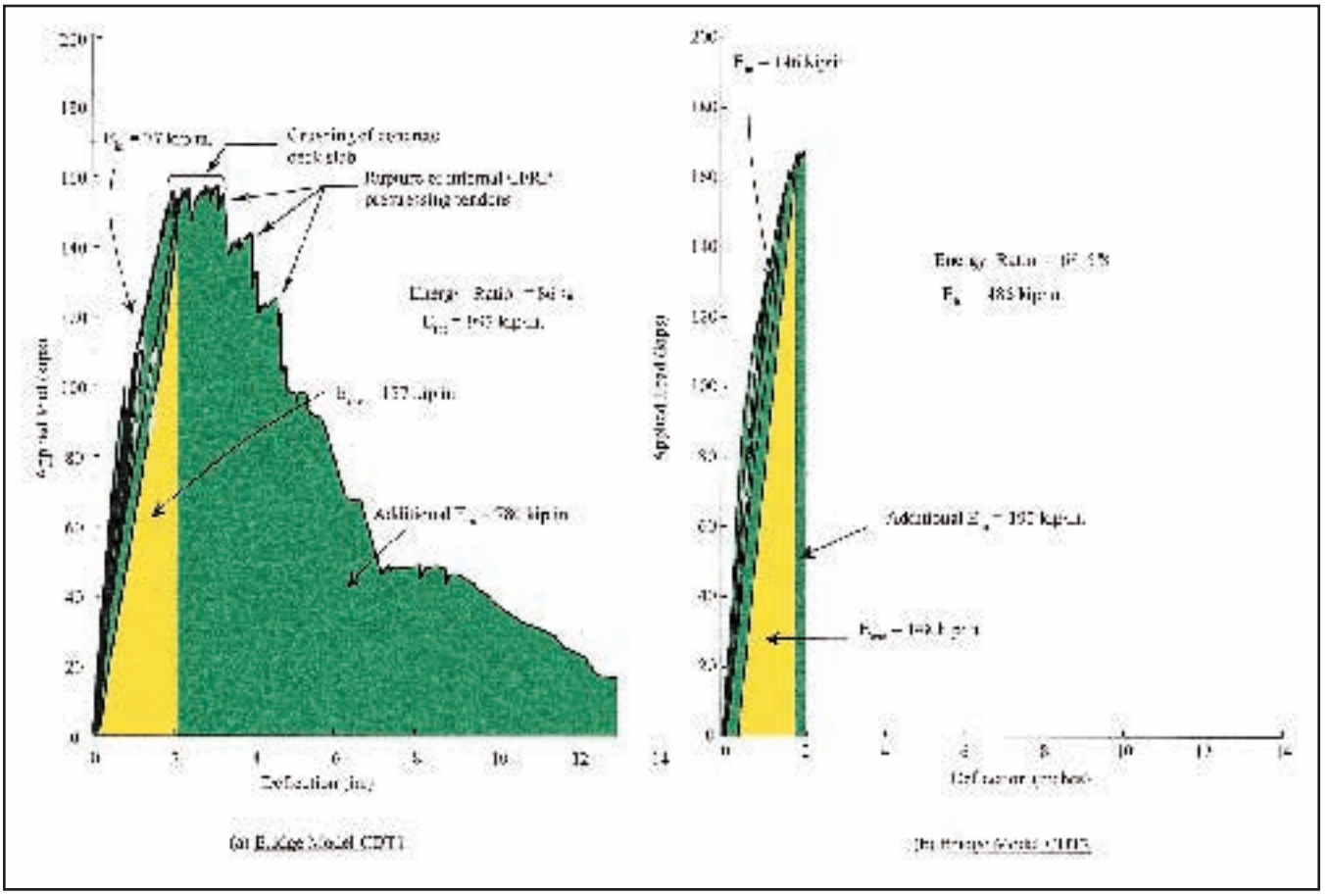

Fig. 16. Energy ratio for Midspan 2.

for Midspan 1 were 80 and 56.5 percent, although these ratios are not shown. Thus, the ductility ratios of Model CDT2 were 23.5 and 16.5 percent lower than those of Model CDT1 for Midspan 1 and Midspan 2, respectively. The reason for this variation arises from a difference in failure modes, as seen in Fig. 16.

Midspan 2 experienced higher deflections than Midspan 1 at each loading stage, for each bridge model. This difference is attributed to the larger repeated load effects on Span 2, which was exposed to a repeated load that was twice the service load. However, it must be noted that for a specific load, the deflection of Model CDT2 was lower than that of Model CDT1.

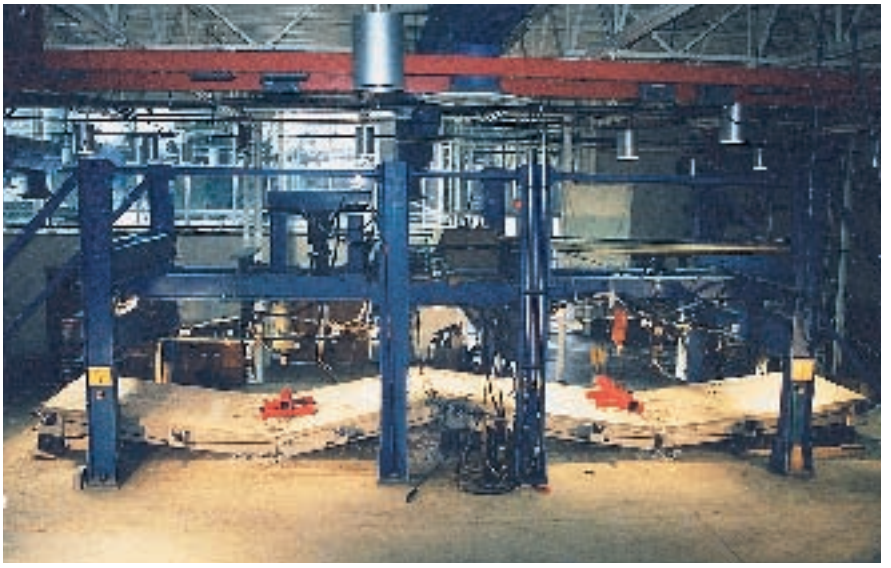

Fig. 17. Failure of Bridge Model CDT1.

The failure of Model CDT1 (see Fig. 17) initiated by crushing of the concrete at the bottom of the webs, while wide transverse cracks formed in the deck slab at the junction of Span 2 and the intermediate support. Note that failure did not occur at the exact center of the intermediate support because of the high stiffness of the bridge at this section (due to the presence of cross-beams and transverse post-tensioned tendons).

Failure at the intermediate support was followed by crushing of the concrete in the deck slab at Midspan 2, then by rupture of the internal Leadline prestressing tendons. Subsequent to the failure of Midspan 2, the loading was continued on Midspan 1. The collapse of Span 1 occurred at a load

of 165 kips (734.3 kN), in a manner similar to that of Span 2.

The failure of Span 2 of Model CDT2 (see Fig. 18) initiated with small flexural cracks forming in the webs. Then, shear failure in the deck slab was followed by wide flexural cracking in one of the exterior webs (at the junction of Span 2 and the intermediate support). This led to the failure of Span 2 at a load of 167 kips (743.2 kN). Subsequent loading caused a similar failure in Span 1 at a load of 183 kips (814.4 kN), on the opposite side of the longitudinal centerline of the bridge.

The failure of both spans of Model CDT2 (see Fig. 18) resulted in a skew symmetric mixed failure mode (flexural failure in the web plus shear failure in the deck slab), near the intermediate support. The main cause of this unexpected failure mode (unlike the failure mode of Model CDT1, which was expected) may be attributed to the unintentional eccentric loading relative to the centerline of both spans.

Figs. 19 and 20 show plan and elevation views of the failure modes of both bridge models. Fig. 20 (Model CDT2) clearly shows the various failure locations and failed components such as the ruptured NEFMAC grids in the deck slab and the ruptured internal prestressing strands. Fig. 19 (Model CDT1) shows similar failures of the NEFMAC grids and the internal prestressing tendons.

Fig. 18. Failure of Bridge Model CDT2.

Fig. 21 shows the response of the post-tensioning forces (with applied static load) in the external draped CFCC strands and CFRP Leadline tendons. Up to a load of about 80 kips (356 kN), there is no variation in the post-tensioning forces of the external strands [see Fig. 21(b)]. However, beyond a load of 80 kips (356 kN), the post-tensioning forces in the CFCC strands increase with the applied static load. This small increase in the post-

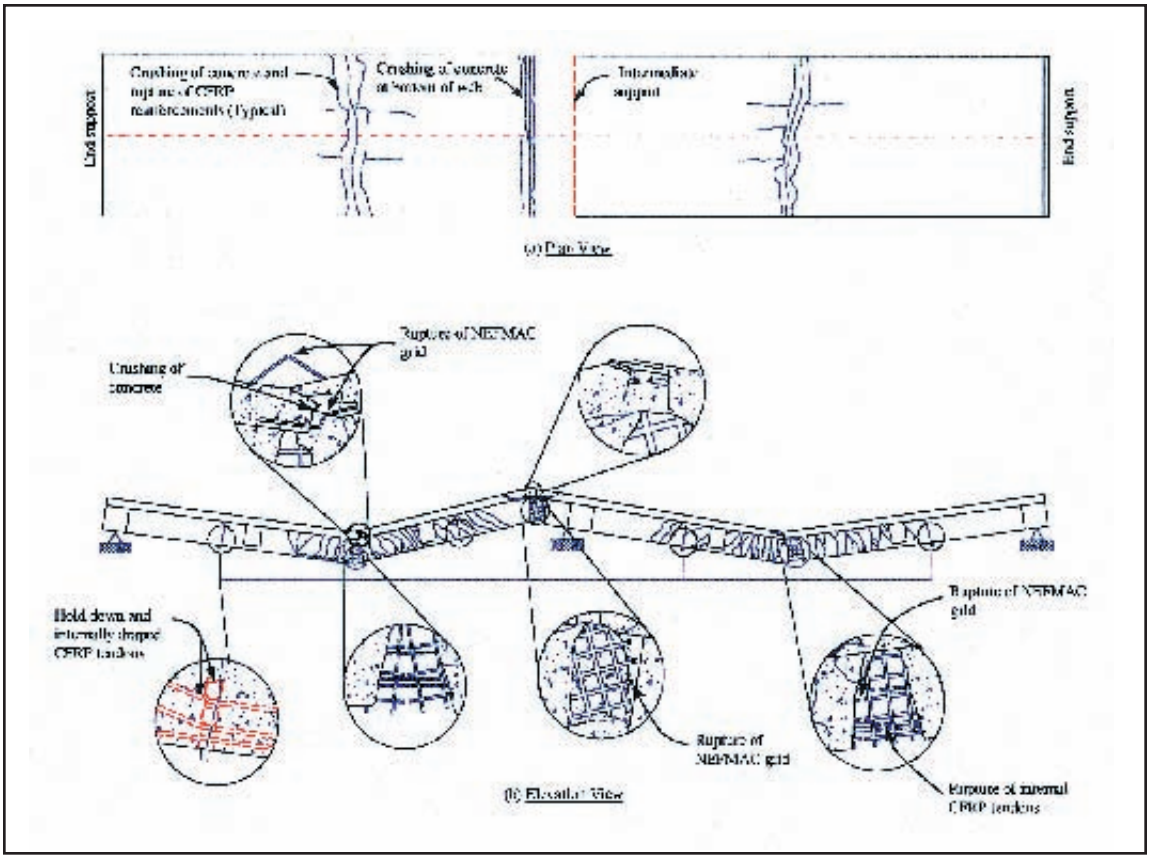

Fig. 19. Failure of Bridge Model CDT1.

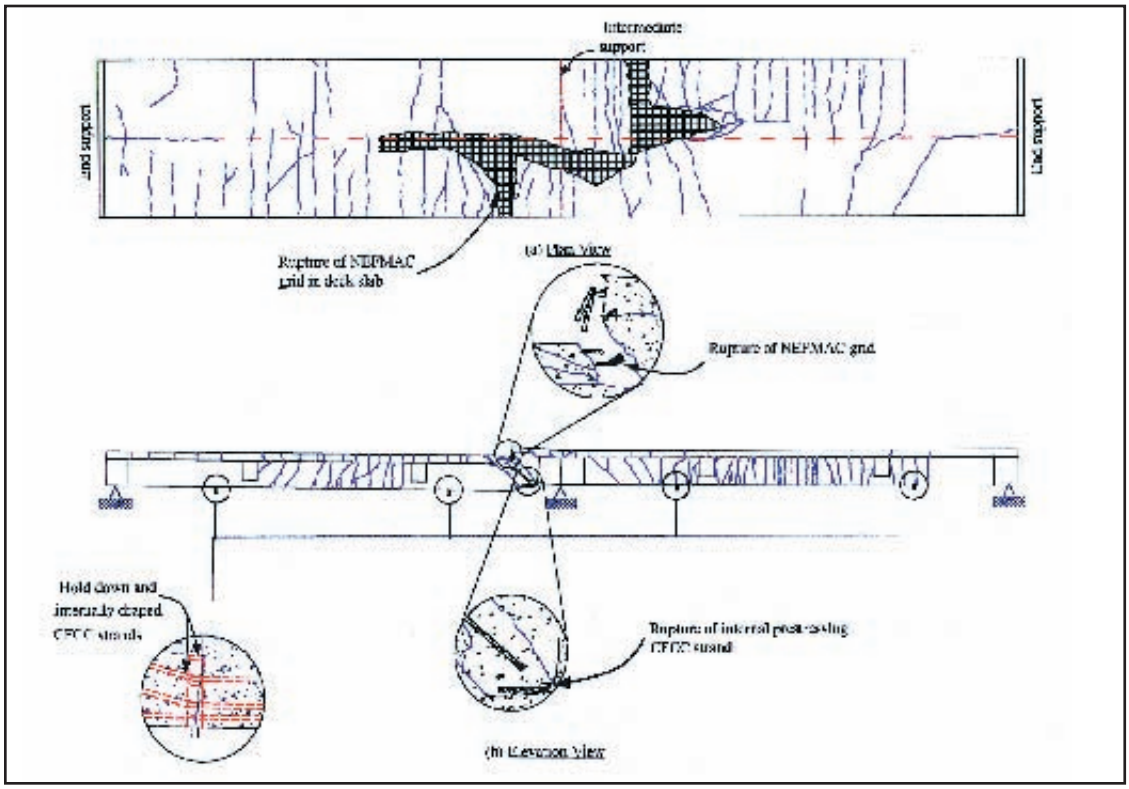

Fig. 20. Failure of Bridge Model CDT2.

tensioning forces is due to large-scale deflection and stretching in the strands.

A similar response is observed in the case of the external CFRP Leadline tendons [see Fig. 21(a)], i.e., the increase in the post-tensioning forces becomes significant during advanced stages of loading, as indicated by the change in the slope of the response curves. Note that at a load close to the ultimate load of Model CDT1, one of the CFRP tendons ruptured, whereas none of the CFCC strands ruptured.

CONCLUSIONS

Based on the results of this investigation, the following conclusions can be drawn:

1. Both Models CDT1 and CDT2 performed very well. There was no significant difference in the responses of the two models with regard to deflection or strain. However, the ductility ratios and ultimate load carrying capacities of Models CDT1 and CDT2 were different, due to their different failure modes. The failure of Model CDT1 occurred in a flexure mode, while the failure of Model CDT2 was characterized as a mixed failure mode (combination of flexure and shear).

2. The ultimate load carrying capacities of Models CDT1 and CDT2 were 162 and 167 kips (721 and 743 kN), respectively. Thus, the difference in load carrying capacities of Models CDT1 and CDT2 was insignificant (less than 5 percent). For a specific load, the deflection of Model CDT2 was less than that of Model CDT1.

3. The ductility of Model CDT2, as measured by the energy ratio, is lower (by 23.5 and 16.5 percent for Midspan 1 and Midspan 2, respectively) than that of Model CDT1.

4. There is no significant effect of static and repeated loads on the post-tensioning forces in the continuous externally draped CFCC strands of Model CDT2, both before and after the post-tensioning adjustment. The same result applies to the post-tensioning forces of the CFRP Leadline tendons of Model CDT1, before and after the post-tensioning force adjustment.

5. The load versus strain relationships for the deck slabs of Models CDT1 and CDT2 show an increase in strain for a specific value of load after an additional 7.5 million cycles of repeated loads, after the post-tensioning force adjustment.

RECOMMENDATIONS

Based on this investigation, the following recommendations can be made:

1. CFRP multiple span continuous prestressed concrete bridges should be prestressed using a combination of pretensioned Leadline tendons and unbonded CFCC strands to achieve their best possible performance.

2. The level of prestressing in the bonded pretensioned Leadline tendons should be limited to 60 percent, whereas the corresponding level of prestressing in the unbonded CFCC strands should be limited to 40 percent. The latter will provide a 30 percent increase (for a total of 70 percent) in prestressing forces in the external continuous unbonded CFCC strands, if restoration or strengthening of the bridge is needed.

3. Three-dimensional NEFMAC grids should be used in both the continuous deck slab and double-tee webs to significantly improve the ductility of continuous bridges.

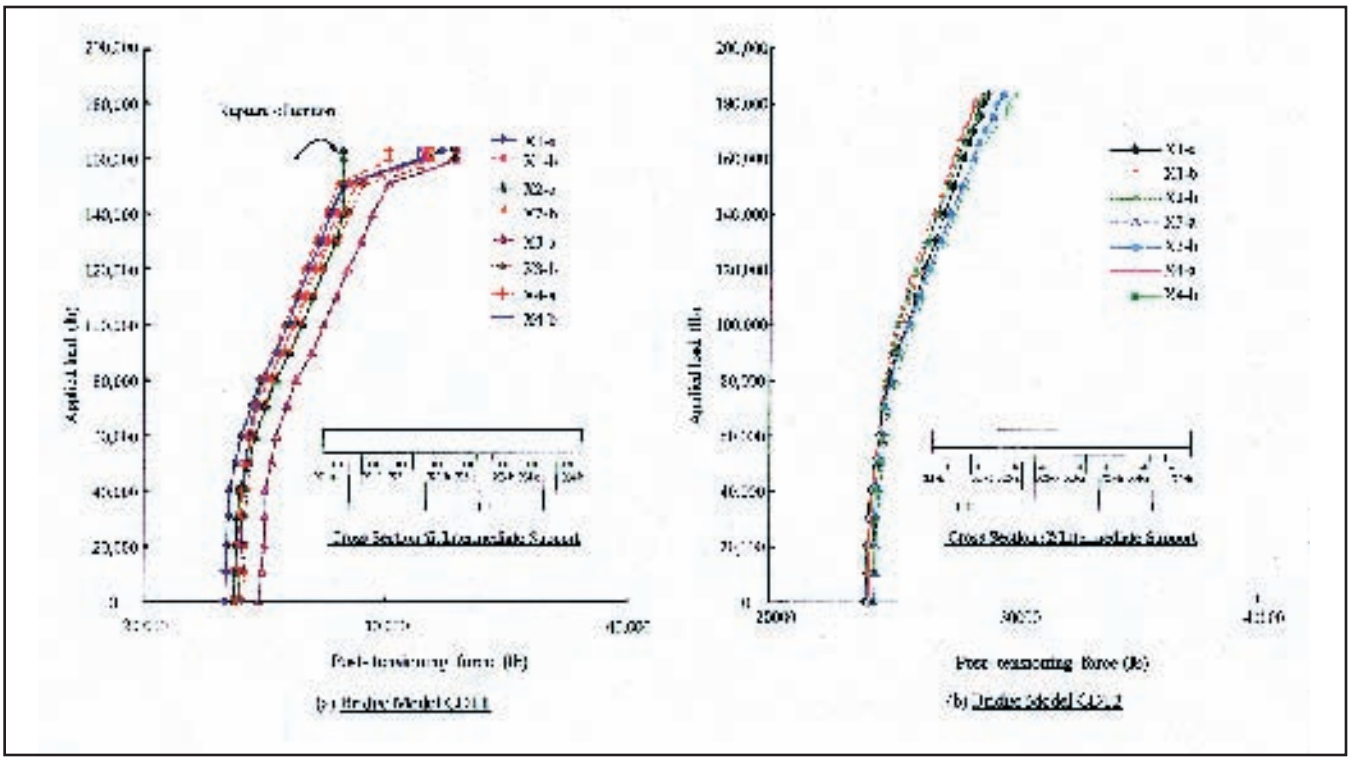

Fig. 21. Response of external tendons/strands during ultimate load test.

ACKNOWLEDGMENTS

This investigation was supported by a consortium of the National Science Foundation (Grant Nos. CMS-9900809 and 9705235), Wright Patterson Air Force Base, Michigan Department of Transportation (MDOT), the Concrete Research Council of the American Concrete Institute, Holnam, Inc., Mitsubishi Chemical Corporation, Sumitomo Corporation, Tokyo Rope Mfg., Inc., and Mitsui Corporation.

This experimental program was made possible through the efforts of several research associates, graduate and undergraduate students. The contributions of N. Blackburn, J. Jerard, and Dr. S. B. Singh are highly appreciated. Technical comments provided by Roger Till (MDOT) are appreciated.

Lastly, the authors want to express their gratitude to the PCI JOURNAL reviewers for their constructive comments.

REFERENCES

1. ACI Committee 440, "State-of-the-Art Report on Fiber Reinforced Plastic (FRP) Reinforcement for Concrete Structures (ACI 440-96)," American Concrete Institute, Farmington Hills, MI, 1996, 153 pp.
2. Rizkalla, S. H., "A New Generation of Civil Engineering Structures and Bridges," Proceedings of the Third International Symposium on Non-Metallic (FRPRC) Reinforcement for Concrete Structures, Sapporo, Japan, V. 1, October 1997, pp. 113-128.
3. Dolan, C. W., "FRP Prestressing in the USA," *Concrete International*, V. 21, No. 10, October 1999, pp. 21-24.
4. Tadros, G., "Provisions for Using FRP in Canadian Highway Bridge Design," *Concrete International*, V. 22, No. 7, July 2000, pp. 42-47.
5. JSCE, "Recommendations for Design and Construction of Concrete Structures Using Continuous Fiber Reinforcing Materials," Concrete Engineering Series 23, Japan Society of Civil Engineers, Tokyo, Japan, October 1997, 325 pp.
6. Grace, N. F., and Abdel-Sayed, G., "Ductility of Prestressed Concrete Bridges Using CFRP Strands," *Concrete International*, V. 20, No. 6, June 1998, pp. 25-30.
7. Grace, N. F., and Abdel-Sayed, G., "Behavior of Externally Draped CFRP Tendons in Prestressed Concrete Bridges," PCI JOURNAL, V. 43, No. 5, September-October 1998, pp. 88-101.
8. Grace, N. F., "Response of Continuous CFRP Prestressed Concrete Bridges Under Static and Repeated Loadings," PCI JOURNAL, V. 45, No. 6, November-December 2000, pp. 84-102.
9. *Leadline™ Carbon Fiber Tendon/Bars*, Product Manual, Mitsubishi Chemical Corporation, Tokyo, Japan, October 1994.
10. NEFMAC, *Technical Data Collection*, Autocon Composites Inc., Canada, 1996, pp. 1-10.
11. Grace, N. F., "Transfer Length of CFRP/CFCC Strands for Double-T Girders," PCI JOURNAL, V. 45, No. 5, September-October 2000, pp. 110-126.
12. Sika CarboDur, *Engineering Guidelines for the Use of Sika CarboDur (CFRP) Laminates for Structural Strengthening of Concrete Structures*, First Edition, Sika Corporation, Lyndhurst, NJ, August 1997.
13. *Technical Data on CFCC*, Product Manual, Tokyo Rope Mfg. Co., Ltd., Tokyo, Japan, October 1993.